

OTHER EXOPLANET'S DETECTION TECHNIQUES

Handbook of Exoplanets (ed. Deeg & Belmonte, 2018). Chapters 32–35.
Exoplanets (ed. Seager, 2010). pp. 79–191.

December 2, 2022

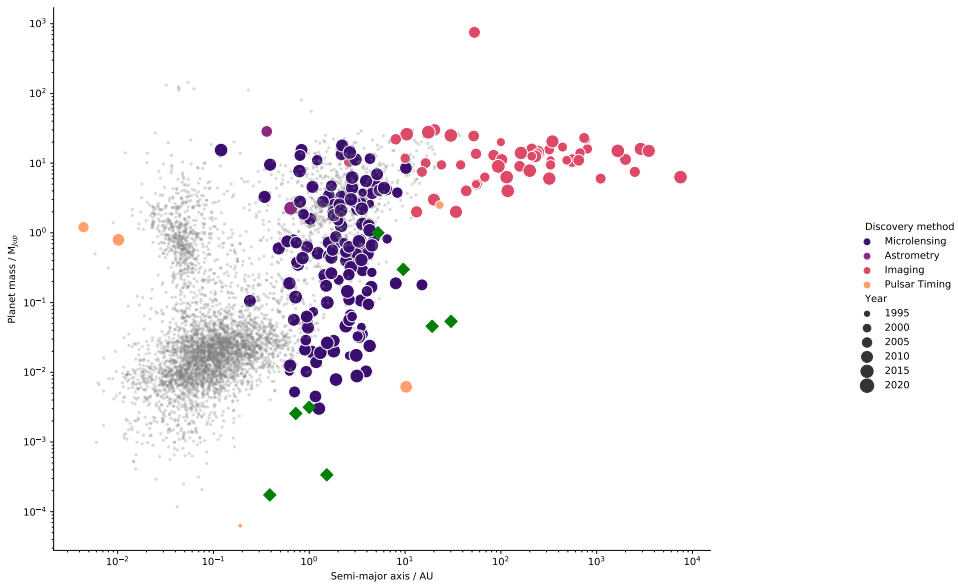
Topics

I. Gravitational Microlensing (141)

II. Astrometry (2)

III. Direct Imaging (61)

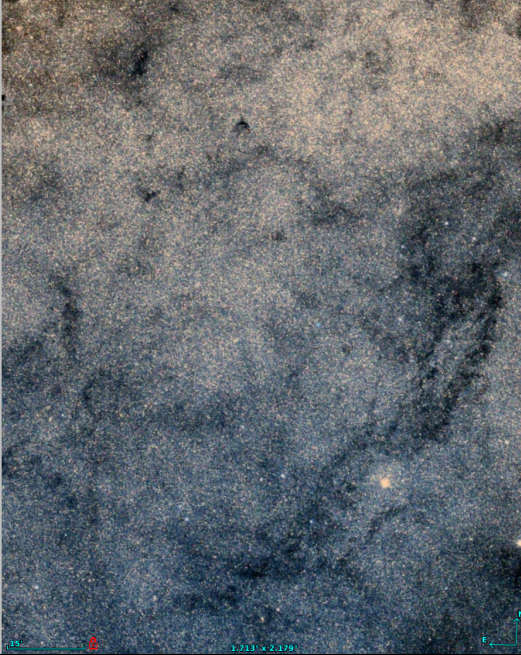
IV. The Fate of Planetary Systems (7)



I. Gravitational Microlensing

- Occurs when a foreground lens happens to pass very close to our line of sight to a more distant background source.
- **Improbable phenomena** → Towards dense stellar fields (OGLE, MOA...)

Galactic centre



Kepler-10



LENS-LIKE ACTION OF A STAR BY THE DEVIATION OF LIGHT IN THE GRAVITATIONAL FIELD

SOME time ago, R. W. Mandl paid me a visit and asked me to publish the results of a little calculation, which I had made at his request. This note complies with his wish.

The light coming from a star A traverses the gravitational field of another star B , whose radius is R_o . Let there be an observer at a distance D from B and at a distance x , small compared with D , from the extended central line \overline{AB} . According to the general theory of relativity, let α_o be the deviation of the light ray passing the star B at a distance R_o from its center.

For the sake of simplicity, let us assume that \overline{AB}

not decrease like $1/D$, but like $1/\sqrt{D}$, as the distance D increases.

Of course, there is no hope of observing this phenomenon directly. First, we shall scarcely ever approach closely enough to such a central line. Second, the angle β will defy the resolving power of our instruments. For, α_o being of the order of magnitude of one second of arc, the angle R_o/D , under which the deviating star B is seen, is much smaller. Therefore, the light coming from the luminous circle can not be distinguished by an observer as geometrically different from that coming from the star B , but simply will manifest itself as increased apparent brightness of B .

The same will happen, if the observer is situated at a small distance x from the extended central line \overline{AB} .

Renn et al., (1997):

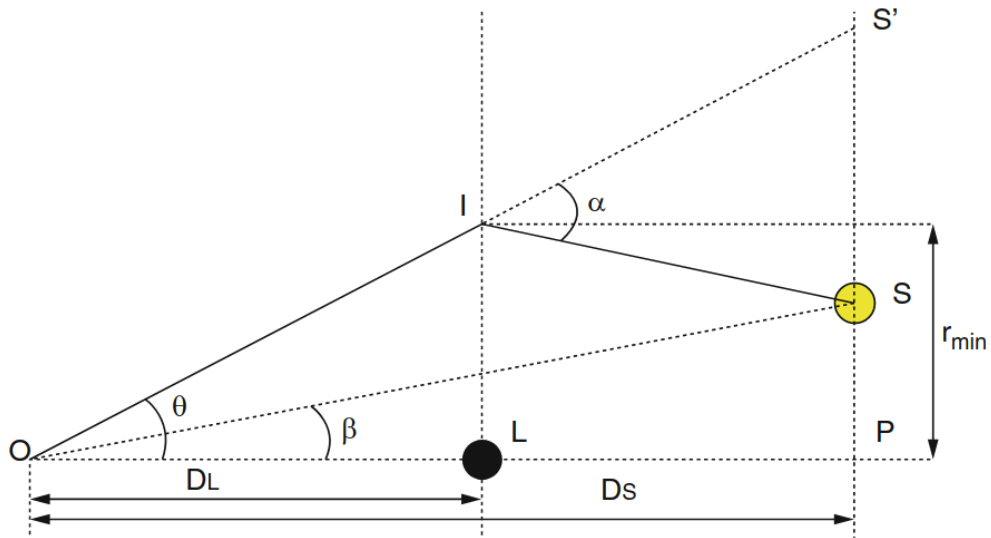
*Reconstruction of some of Einstein's research notes dating back to **1912** reveals that he explored the possibility of gravitational lensing 3 years before completing his general theory of relativity.*

Theoretical advances: Refsdal (1964) and Paczynski (1986)

Towards exoplanets: Mao & Paczynski (1991) and Gould & Loeb (1992)

Current microlensing searches:

1. OGLE - Optical Gravitational Lensing Experiment
2. KMT - Korea Microlensing Telescope Network
3. MOA - Microlensing Observations in Astrophysics



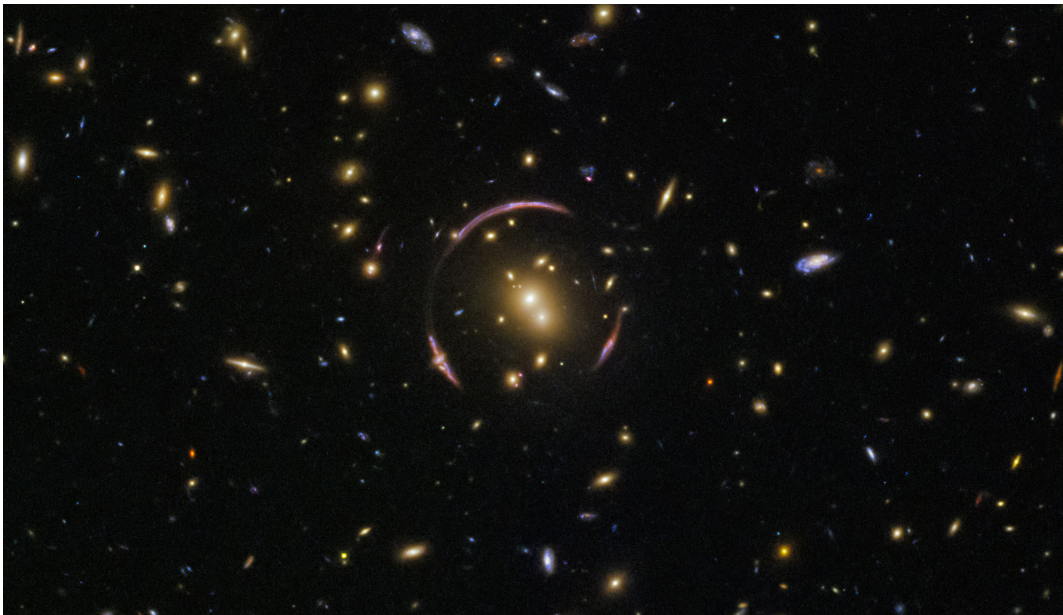
Principle: Light coming from S (source) is deflected by an angle α when it passes through the gravitational field generated by a **point-like** mass L (lens) creating an *illusion* for the observer O that the source is at the position I (image) in the lens plane.

Lens equation (Schneider & Weiss, 1992):

$$\alpha(D_S - D_L) = \theta D_S - \beta D_S; \quad \alpha := \frac{4GM}{c^2 D_L \theta}. \quad (1)$$

Einstein ring:

$$\theta_E = \sqrt{\frac{4G}{c^2} M \frac{D_S - D_L}{D_S D_L}} = \sqrt{\frac{2R_{\text{sch}}}{D_{\text{rel}}}}; \quad D_{\text{rel}} = (D_S^{-1} - D_L^{-1})^{-1}. \quad (2)$$





In practical quantities,

$$\theta_E = 550 \mu\text{as} \left(\frac{M}{0.3 M_\odot} \right)^{1/2} \left(\frac{\pi_{\text{rel}}}{125 \mu\text{as}} \right)^{1/2}, \quad (3)$$

which corresponds to a physical Einstein ring radius at the distance of the lens of Gaudi, 2010

$$r_E = \theta_E D_L = 2.2 \text{AU} \left(\frac{M}{0.3 M_\odot} \right)^{1/2} \left(\frac{D_S}{8 \text{kpc}} \right)^{1/2} \left[\frac{x(1-x)}{0.25} \right]^{1/2}; x \equiv \frac{D_L}{D_S} \quad (4)$$

Define, for simple lens, $u \equiv \beta/\theta_E$, $z \equiv \theta/\theta_E$. The lens equation is found to be

$$u = z - \frac{1}{z} \quad \longrightarrow \quad \mathbf{z^2 - uz - 1 = 0} \quad (5)$$

In case of imperfect alignment ($u \neq 0$), two images are formed at positions

$$z_{\pm} = \pm \left(\frac{\sqrt{u^2 + 4} \pm u}{2} \right) \quad (6)$$

Lens magnification:

$$A_{\pm} = \frac{z_{\pm}}{u} \frac{dz_{\pm}}{du} = \frac{1}{2} \left(\frac{u^2 + 2}{u\sqrt{u^2 + 4}} \pm 1 \right) \longrightarrow \mathbf{A(u) = \frac{u^2 + 2}{u\sqrt{u^2 + 4}}} \quad (7)$$

Problem #1: Show that $\lim_{u \rightarrow \infty} (A_+, A_-) = (1, 0)$, and that $\lim_{u \ll 1} A \sim u^{-1}$

Consider now N_L **objects**, with total mass $M = \sum m_i$. And let θ_i be the two-dimensional coordinates of these individual masses in the lens plane.

$$\alpha(\theta) = \frac{4G}{c^2} \left(\frac{1}{D_L} - \frac{1}{D_S} \right) \sum m_i \frac{\theta - \theta_i}{|\theta - \theta_i|^2}. \quad (8)$$

Take the complex representations for the source $u = \xi + i\eta$ and image $z = x + iy$ positions (Witt, 1990). The lens equation becomes

$$u = z - \sum_i^{N_L} \frac{m_i}{M} (\bar{z} - \bar{z}_i)^{-1} \quad (9)$$

The **magnification** can be greater or less than 1, being equal to the inverse of the Jacobian matrix determinant

$$A_j = \frac{1}{\|J\|} \Big|_{z=z_j}, \quad \|J\| = 1 - \partial_z u \bar{\partial}_z \bar{u} \quad (10)$$

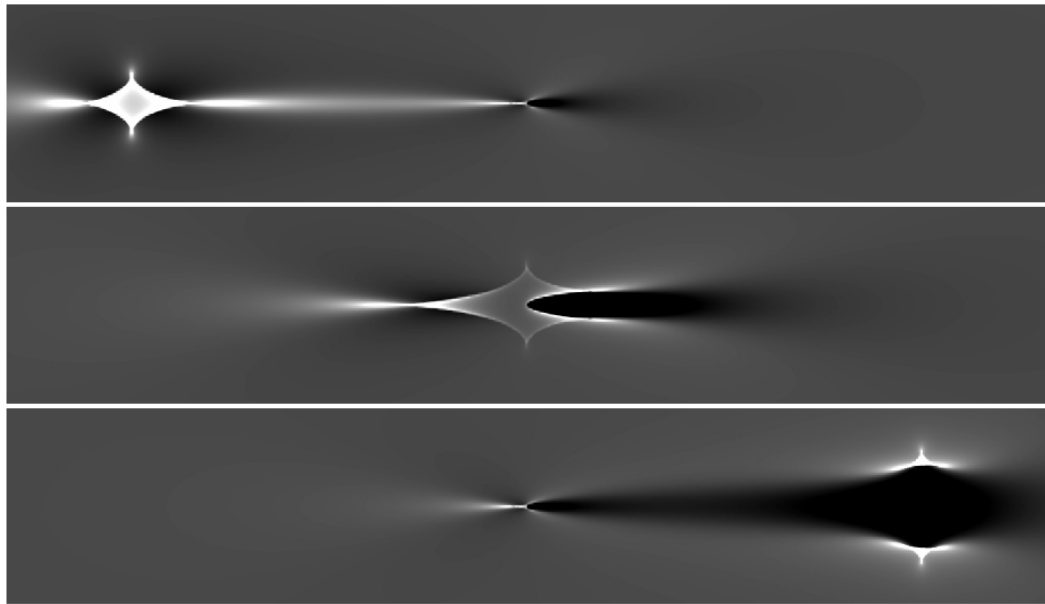
Singularities occur for positions where $\|J\| = 0$ ¹. In practice, S cannot be considered point sources, and these singularities appear as *very high but finite magnifications*.

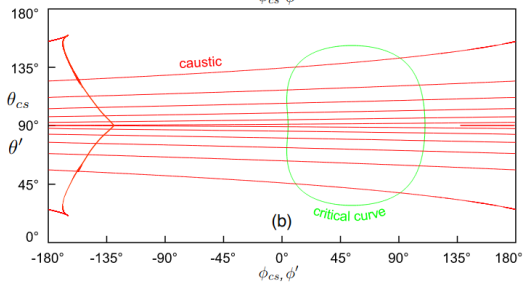
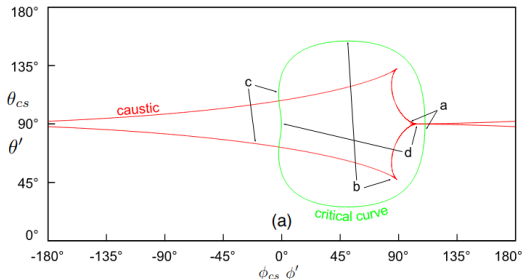
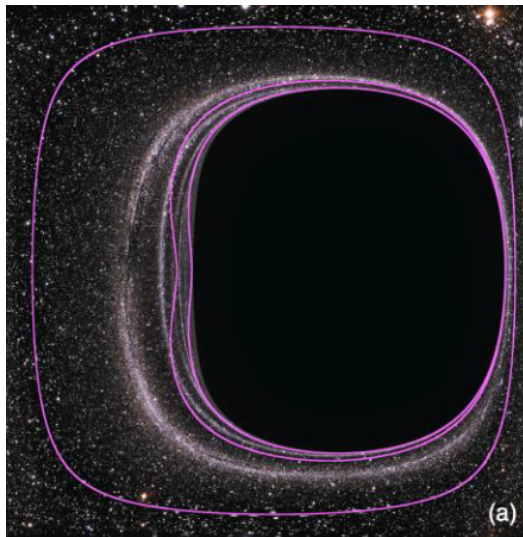
From Eq. (9), $\overline{\partial_z u} = \sum \left[\varepsilon_i / (\bar{z}_i - \bar{z})^2 \right]$, and according to Eq. (10), $\|J\| = 0$ positions are given by

$$\left| \sum_i^{N_L} \frac{\varepsilon_i}{(\bar{z}_i - \bar{z})^2} \right| = 1. \quad (11)$$

Solutions of Eq. (11) shape as closed contours in the lens plane, known as **critical curves**

¹ *Why your mental map of the world is (probably) wrong*





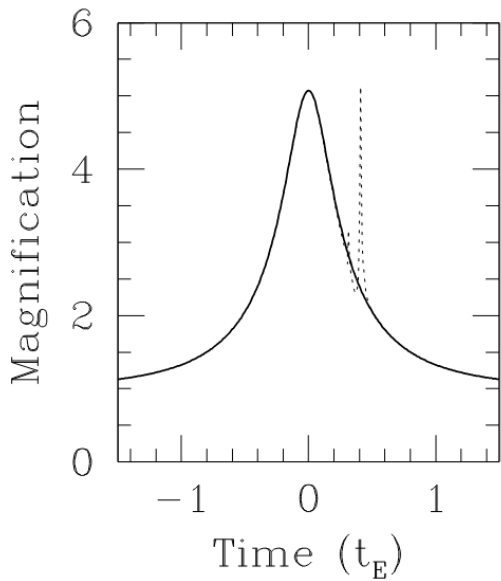
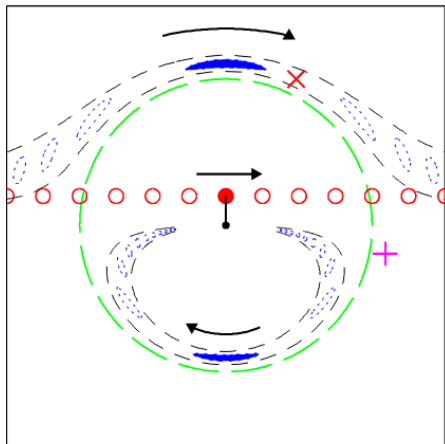
James et al., (2014). *Gravitational Lensing by Spinning Black Holes in Astrophysics, and in the Movie Interstellar*

The lens, source, and observer are in motion. Therefore, $\theta_E = \theta_E(t)$, and $A = A(t)$. In case of uniform rectilinear motion

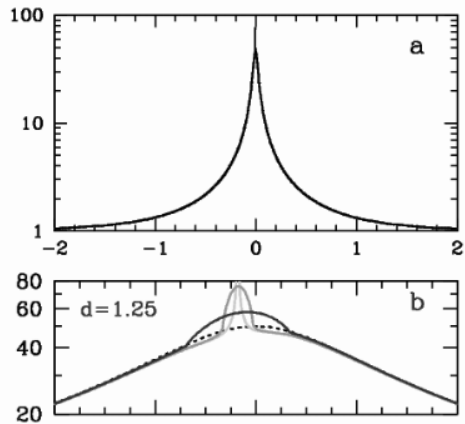
$$u(t) = \left[u_0^2 + \left(\frac{(t - t_0)}{t_E} \right)^2 \right]^{1/2} ; \quad u_0 = \min(D_S, D_L), \quad t_0 = t(u = u_0). \quad (12)$$

where t_E is the timescale to cross the angular Einstein ring radius (in the order of **a month** for events toward the Galactic bulge (Gaudi, 2010)).

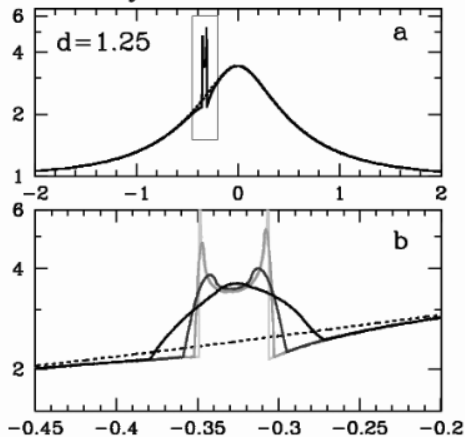
$$t_E = 19\text{days} \left(\frac{M}{0.3M_\odot} \right)^{1/2} \left(\frac{\pi_{\text{rel}}}{125\mu\text{as}} \right)^{1/2} \left(\frac{\pi_{\text{rel}}}{10.5\text{mas/yr}} \right)^{-1} \quad (13)$$

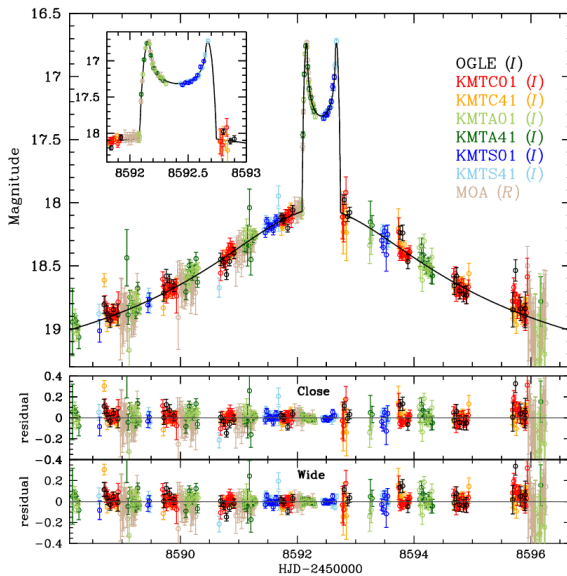


Central Caustic Perturbations



Planetary Caustic Perturbations





KMT-2019-BLG-0371 ($M_p = 7.70 M_{\text{Jup}}$).

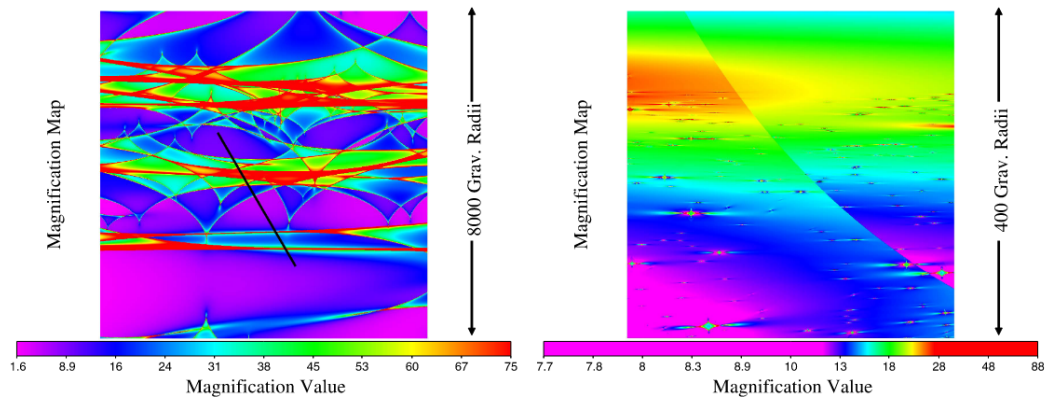


Figure 2. (Left) Microlensing magnification map of RXJ 1131–1231A with only stars and a dimension of $(8000 r_g)^2$. A random track ($3740 r_g$) for a compact source moving across the map with a 10 year duration is overplotted. The probability for a caustic to land on the source region is only a few percent, significantly below the observed rate of $\sim 30\%$. (Right) Magnification map, with a dimension of $(400 r_g)^2$, with the additional planet population and a planet mass-fraction of $\alpha_{pl} = 0.001$ for RXJ 1131–1231A. The caustic density is much higher with the additional planets.

II. Astrometry

Principle: Observations of their parent stars orbiting the common centre of mass; measuring the two coordinates in the plane of the sky²

$$\theta = \frac{m}{M} \frac{a}{d} = 3\mu\text{as} \left(\frac{m}{M_{\odot}} \right) \left(\frac{M}{M_{\odot}} \right)^{-2/3} \left(\frac{P}{\text{yr}} \right)^{2/3} \left(\frac{d}{\text{pc}} \right)^{-1} \quad (14)$$

²Remember **Laboratory 04!**

Orbital fit:

The position of a star in the sky over time is given by: $P, T_0, e, \theta, \Omega, \omega, i, a$.

Non-linear least-squares fit of a model describing the motion of the star to the data (including parallax and proper motion):

$$\xi(t) = \alpha_0^* + \Pi_{\alpha^*} \bar{\omega} + (t - t_0) \mu_{\alpha^*} + BX(t) + GY(t), \quad (15)$$

$$\eta(t) = \delta_0 + \Pi_{\delta} \bar{\omega} + (t - t_0) \mu_{\delta} + AX(t) + FY(t). \quad (16)$$

$$\alpha^* = \alpha \cos \delta, \mu_{\alpha} = \mu_{\alpha} \cos \delta$$

Thiele-Innes constants

$$A = \theta(\cos \omega \cos \Omega - \sin \omega \sin \Omega \cos i) \quad (17)$$

$$B = \theta(\cos \omega \sin \Omega - \sin \omega \cos \Omega \cos i) \quad (18)$$

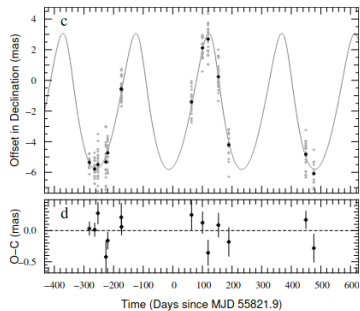
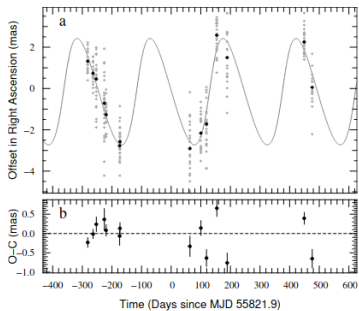
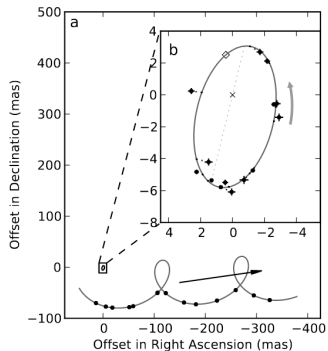
$$F = \theta(-\sin \omega \cos \Omega - \cos \omega \sin \Omega \cos i) \quad (19)$$

$$G = \theta(-\sin \omega \sin \Omega + \cos \omega \cos \Omega \cos i) \quad (20)$$

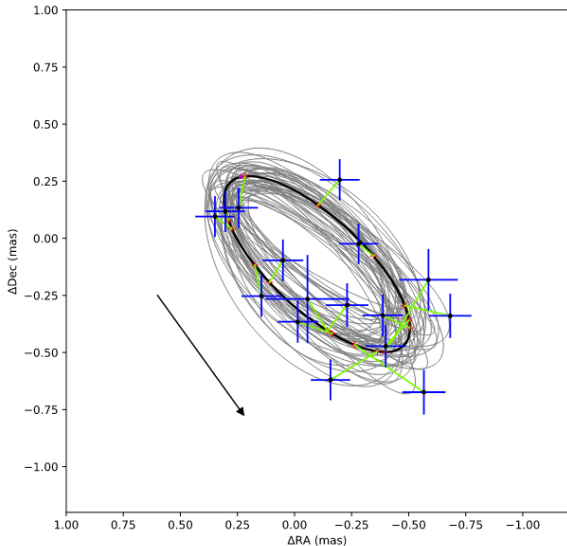
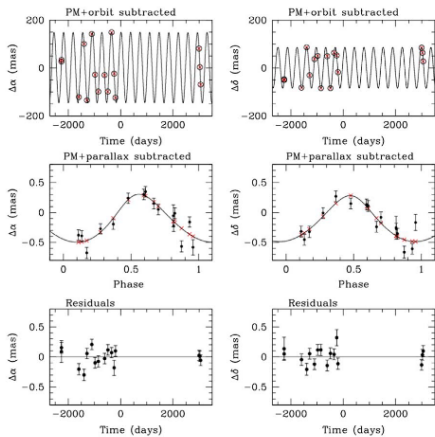
with $X(t)$ and $Y(t)$ describing the motion of the star in its orbit (solution of **Kepler's equation** ($E = (2P/\pi)(t - T) + e \sin E$)).

$$X(t) = \cos E - e \quad (21)$$

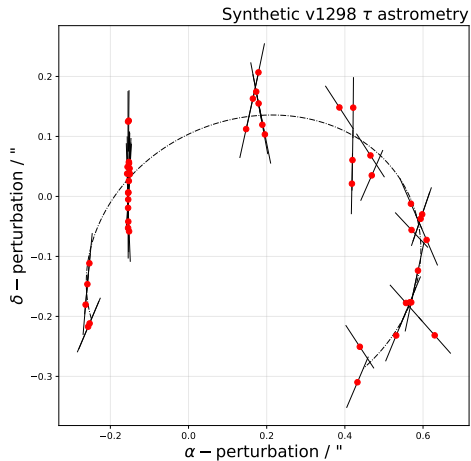
$$Y(t) = \sqrt{1 - e^2} \sin E \quad (22)$$



DENIS-P J082303.1-491201b – L1.5 dwarf ($M = 28.5 \pm 1.9 M_{\text{Jup}}$; Sahlmann+2013)

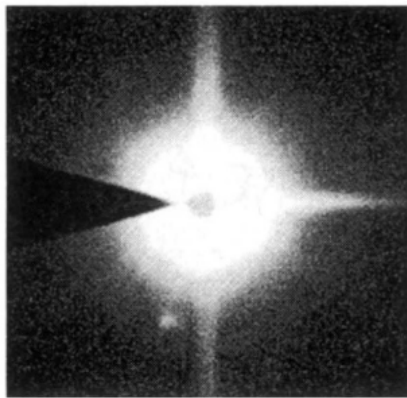
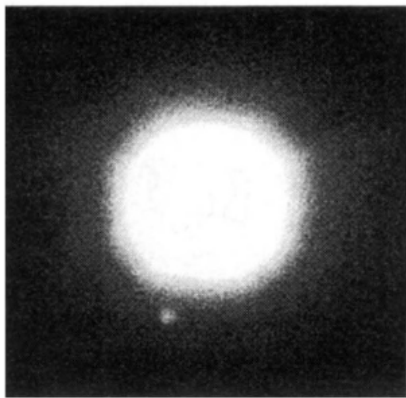


GJ 896Ab ($M = 2.3 M_{\text{Jup}}$; Curiel+2022)

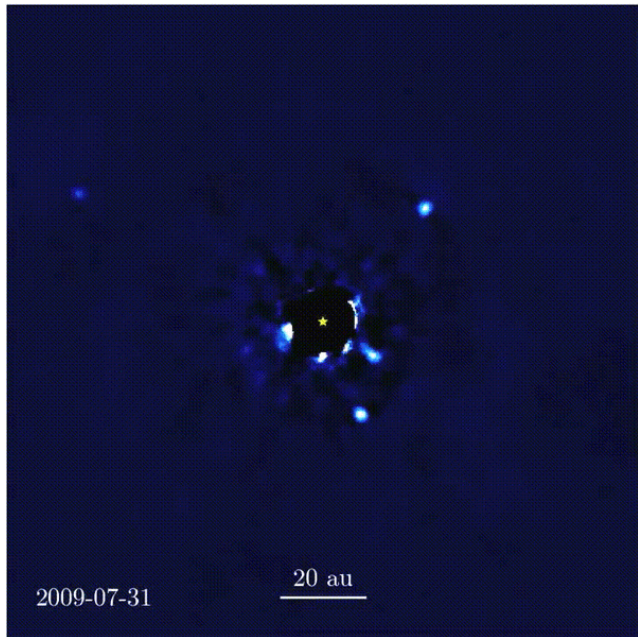


III. Direct Imaging:

- Brown & Burrows (1990) - Earliest theoretical works
- Gliese 229b (Nakajima et al., 1995; Oppenheimer et al., 1995) - 1st obj. imaged



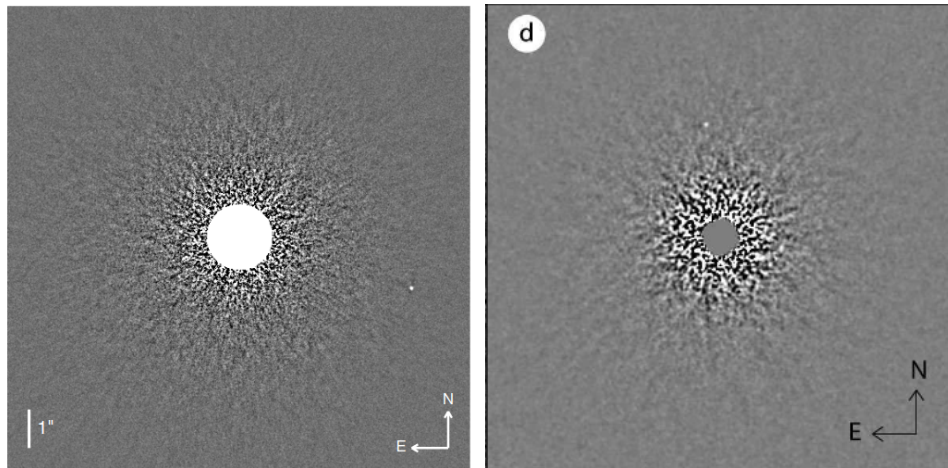
As a brown dwarf, its core temperature is high enough to initiate the fusion of deuterium with a proton to form helium-3, but it is thought that it used up all its deuterium fuel long ago.



2009-07-31

20 au

- Faint companions (BD, etc.) - Lafrenière et al., (2007), Biller et al., (2007), Metchev & Hillenbrand (2009), Vigan et al., (2012), Brandt et al., (2014)



HIP 10670 (A1V, 10^8 Gyr, $T = 9440$ K) and HD 691 (K0V, $T = 5633$ K)

Coronagraph: To use a series of optical devices to shape the telescope response so that it varies as the position of a source changes in the sky.

$$F_{\lambda}(\beta) = F_{\text{star},\lambda}(\beta) + F_{\text{planet},\lambda}(\beta - \alpha_p) \quad (23)$$

$\beta = 2\text{-D angular sky coordinates}$, $\alpha_p = \text{angular distance between star and planet}$.

The image will be (Roddier, 1981)

$$R_{\lambda_0}^{\text{T}}(\beta) \star F_{\lambda_0}(\beta)|_{\alpha} \quad (24)$$

with $R_{\lambda_0}^{\text{T}}(\beta)$ is the response of the telescope and atmospheric effects.

Assume that the deterministic response of the telescope is known, then the noise at the planet's position in a long exposure time (T_{exp}) is given by (e.g., McLean, 2008)

$$\sqrt{[f_{\text{star}}R^\top(\alpha_p) + f_{\text{planet}}R^\top(0)]T_{\text{exp}}} \quad (25)$$

Consequently, the SNR is

$$\text{SNR} = \frac{1}{\sqrt{1 + \frac{f_{\text{star}}R^\top(\alpha_p)}{f_{\text{planet}}R^\top(0)}}} \sqrt{f_{\text{planet}}R^\top(0)T_{\text{exp}}} \quad (26)$$

Note, having the planet very close to the star means an incredibly large increase of exposure time

$$\frac{T_{\text{exp},\alpha_p}}{T_{\text{exp},\infty}} \sim \frac{f_{\text{star}}R^\top(\alpha_p)}{f_{\text{planet}}R^\top(0)} \quad (27)$$

Example:

Hubble takes 1 hour at $\lambda = 500$ nm to acquire SNR ~ 5 of a 27 mag galaxy.
Consider taking an image of Jupiter (~ 5 AU) around a 4.5 mag star at 10 pc.

$$\alpha_p = 10\lambda/D.$$

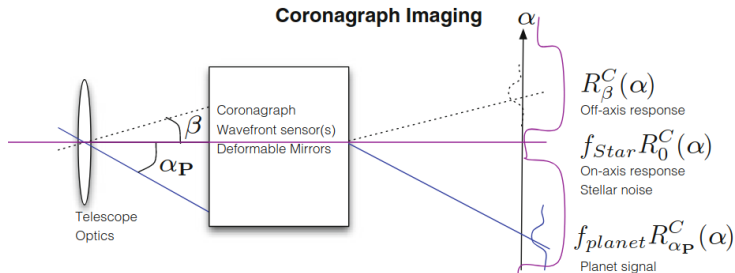
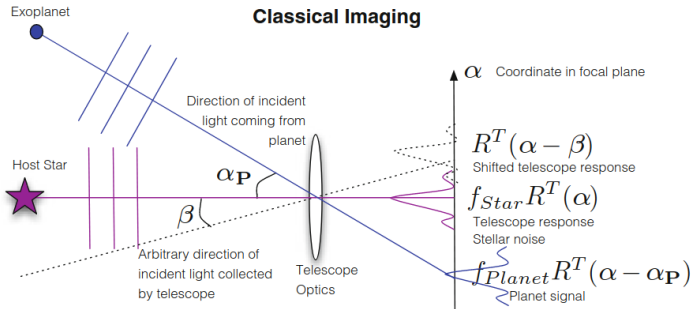
Assume that HST response is similar to the one of a circular aperture³,

$$R^\top(\alpha_p)/R^\top(0) \sim 0.01.$$

Since $f_{\text{star}}/f_{\text{planet}} \sim 10^9$, to achieve a SNR ~ 5 would require **~ 1100 years!**

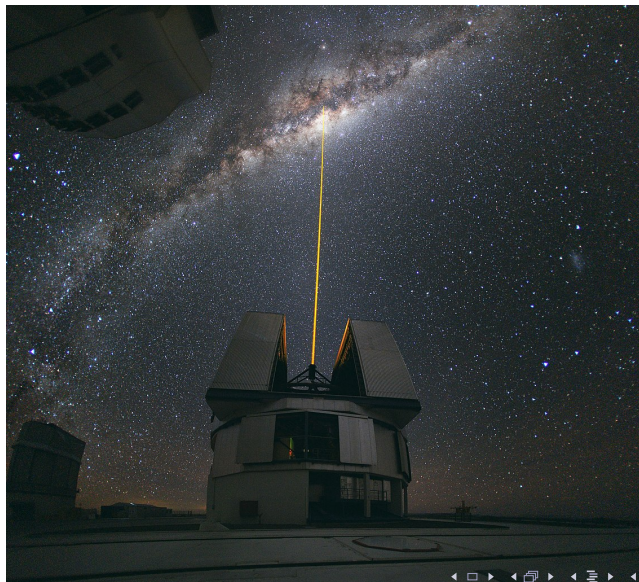
Luckily: Starlight suppression techniques

³Airy function



Adaptive Optics (AO): (Watson, 1997).

Correct time-dependent optical imperfections → **Atmospheric turbulence.**



Under an extreme regime (Ex-AO), for which the residual phase is much smaller than a radian, the incident field is given by

$$\varphi_{\text{AO}}(u) = 1 + i\phi_{\text{res}}(u), \quad (28)$$

Classical imaging responses⁵ are given by the time average $\langle R(\beta) \rangle \star F_\lambda(\beta)$. In the Fourier space,⁶ from which the imaging response becomes⁷

$$\langle R(\alpha) \rangle = \mathcal{F}[\langle \phi(u)\phi(u + \nu)^\dagger \rangle](\alpha) \star R^\text{T}(\alpha) \quad (29)$$

In the case of Kolmogorov (1941) atmospheric turbulence⁸,

$$\langle \phi(u)\phi(u + \nu)^\dagger \rangle = \exp\left(-3.44\lambda \left|\frac{\nu}{r_0}\right|^{5/3}\right) \quad (30)$$

⁵Davis, J.E. (2001). *In-depth mathematical description of the response functions (X-ray data)*

⁶Use the Wiener-Khinchin theorem and the fact that FTs are linear concerning time average.

⁷ $\phi(u)$ does not depend on β since exoplanet imaging occurs over a small field of view.

⁸ r_0 is the Fried parameter that describes the characteristic scale of the turbulence

(28) \rightarrow (29):

$$R_{\text{AO}}(\alpha) = R^{\text{T}}(\alpha) + \mathcal{F}[\langle \phi_{\text{res}} \phi_{\text{res}}(u + \nu) \rangle](\alpha) \star R^{\text{T}}(\alpha), \quad (31)$$

assuming that the residual wavefront errors are zero mean ($\langle \phi_{\text{res}}(u) = 0 \rangle$).

Adding a coronagraph (see Herscovici-Schiller et al., 2017), it is replaced the convolution with a field-dependent integral, and assume $\langle \phi_{\text{res}}(u) = 0 \rangle$. The stellar and planet responses will be⁹

$$R_0^{\text{C+AO}}(\alpha) = R_0^{\text{C}}(\alpha) + \int |\widehat{\phi_{\text{res}}}|^2(\beta) R_{\beta}^{\text{C}}(\alpha) d\beta \quad (32)$$

$$R_{\alpha_p}^{\text{C+AO}}(\alpha) = R_{\alpha_p}^{\text{C}}(\alpha) + \int |\widehat{\phi_{\text{res}}}|^2(\beta) \star R_{\beta - \alpha_p}^{\text{C}}(\alpha) d\beta \quad (33)$$

⁹Using again the Wiener-Khinchin theorem to replace the autocorrelation of the phase residuals by their power spectral density (PSD) $|\widehat{\phi_{\text{res}}}|^2(\alpha)$.

Current and Future Projects

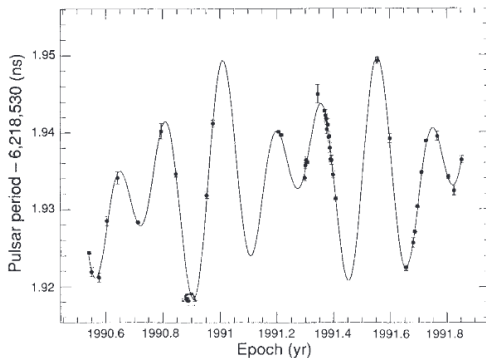
1. Large Binocular Telescope Interferometer (LBTI; Hinz, 2009)
To detect Jupiter-like planets around young (< 2 Gyr) stars.
2. Gemini Planet Imager (GPI; Macintosh et al., 2008);
Images and spectra of ~ 100 -200 young planets.
3. Spectro-Polarimetric High-Contrast Exoplanet Research (SPHERE; Beuzit et al., 2008)
Several tens of warm and young Jupiter-like planets.;
4. Thirty Meter Telescope (TMT)
Skidmore et al., 2015
Giant Magellan Telescope (GMT)
GMT Science Book (2018)
European Extremely Large Telescope (E-ELT)
E-ELT Science Publication (ESO Website)
5. Large UV/Optical/IR Surveyor (LUVOIR)

IV. Planets Around Stellar Remnants

Pulsars¹⁰:

Rotating neutron star remnants from supernovae of $\geq 8 M_{\odot}$ stars.

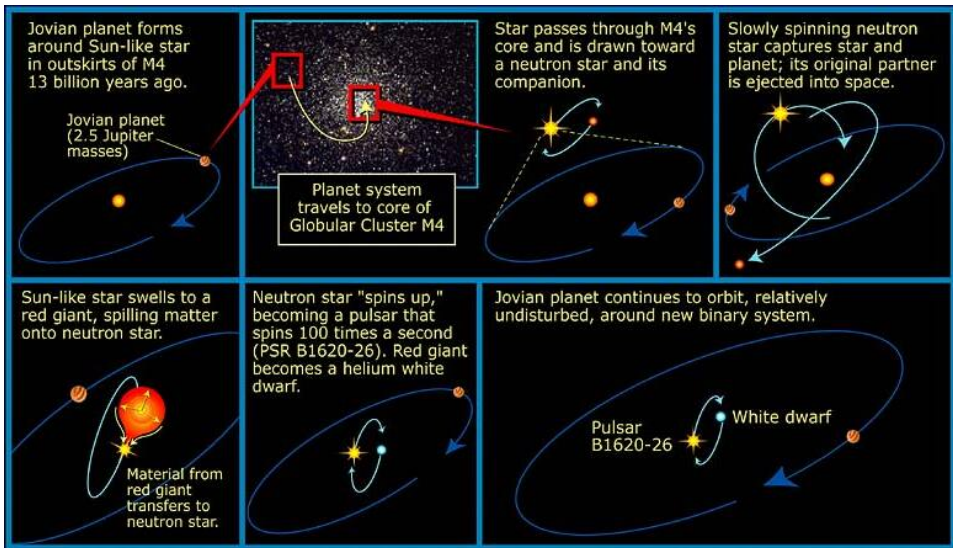
PSR B1257+12b: First exoplanet ever discovered (Wolszczan and Frail, 1992)¹¹



¹⁰A review about General Relativity: Backer & Hellings, 1986

¹¹Arecibo radiotelescope (RIP); 2.8, 3.4 M_{\oplus} at $P = 98.2$ and 66.6 d.)

PSR B1620-26 (One of the oldest known exoplanet; Thorsett et al., 1999)



In **exoplanet context**, it relies on the modelling of planetary orbits based on precise measurements of a varying Römer delay of time-of-arrival (TOA) of the pulsar pulses $t_R = \Delta z/c$ due to the changing line-of-sight projection Δz of the reflex motion of a pulsar.

$$\text{No. of pulses : } \phi_i = \int_{t_0}^t \frac{1}{P(t)} dt; \quad \nu(t) = 1/P(t) = \text{rotation frequency.} \quad (34)$$

Spindown process¹²

(34) can be parameterised in terms of the rotation frequency and time derivatives as a Taylor series¹³

$$\phi_i = \phi_0 + \nu t_i + \frac{1}{2} \dot{\nu} t_i^2 + \frac{1}{6} \ddot{\nu} t_i^3 + \mathcal{O}(t^4) \quad (35)$$

¹²Read about the Shklovskii (1970) effect.

¹³PSR B1620-26 was discovered from a precise timing analysis of the dynamical *contamination* of the higher-order period derivatives (Joshi & Rasio, 1997).

Since the Earth is in motion, it is necessary to correct the TOAs to the Solar System barycentre (SSB)

$$t_B = t_{\text{obs}} + t_{\text{clk}} - \frac{(\mathbf{r} \times \mathbf{n})}{c} - \frac{D'}{f^2} + t_{S\odot} + t_{E\odot} + t_R \quad (36)$$

where,

t_{clk} = net clock correction that has to be applied to t_{obs}

r = observations

n = unit vector in the pulsar direction

f = observed frequency

$t_{S\odot}$ = delay acquired while prop. through the Schwarzschild space in the S.S.

$t_{E\odot}$ = combined effect of gravitational redshift and time dilation in the Solar System

t_R = additional Römer delay due to a Keplerian orbital motion

Keplerian orbital motion:

$$V_r = \frac{2\pi a_1 \sin i}{P_b \sqrt{1 - e^2}} [\cos(\omega + \nu) + e \cos \omega] \quad (37)$$

The observed period of an orbiting pulsar will be Doppler-shifted following

$$P = P_0 \left(1 + \frac{V_r}{c} \right) \quad (38)$$

Consequently, it is possible to model t_R following¹⁴

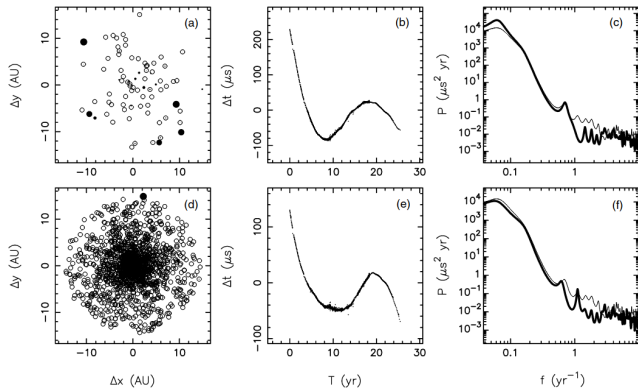
$$t_R = \left(\frac{a_1 \sin i}{c} \right) (\cos E - e) \sin \omega + \left(\frac{a_1 \sin i}{c} \right) \sin E \sqrt{1 - e^2} \cos \omega. \quad (39)$$

¹⁴see eq. (2.30) in Blandford & Teukolsky (1976).

In practice, for a circular orbit, $i = \pi/2$, and $m_1 = 1.35 M_\odot$

$$t_R \sim 0.5s \left(\frac{a_2}{1 \text{ AU}} \right) \left(\frac{m_2}{M_{\text{Jup}}} \right) \left(\frac{m_1}{M_\odot} \right)^{-1} \quad (40)$$

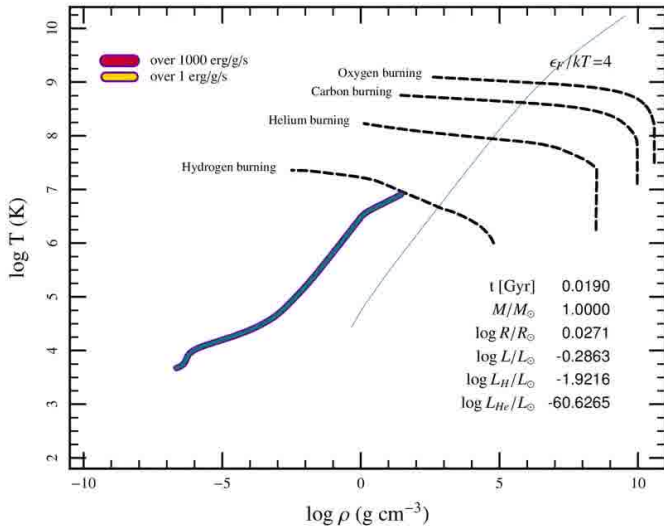
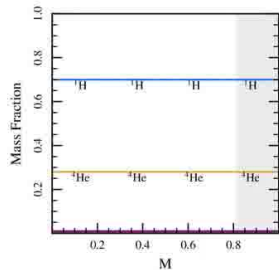
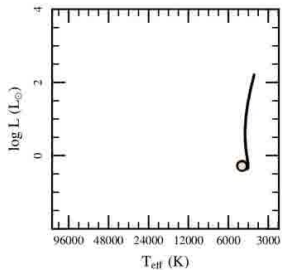
Large asteroid-mass bodies in long-period orbits would be detectable¹⁵.

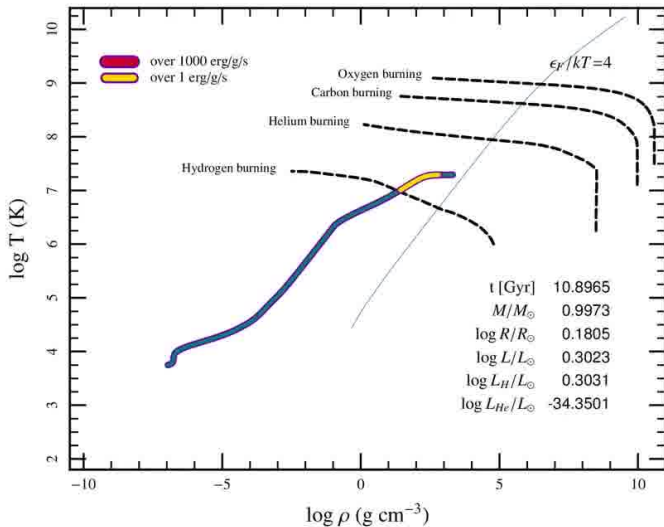
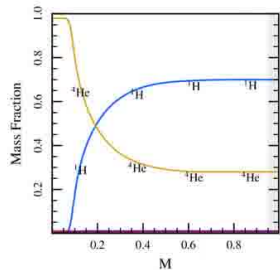
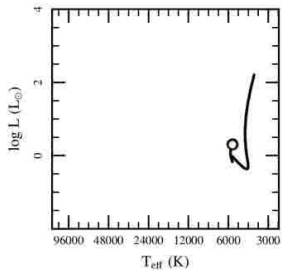


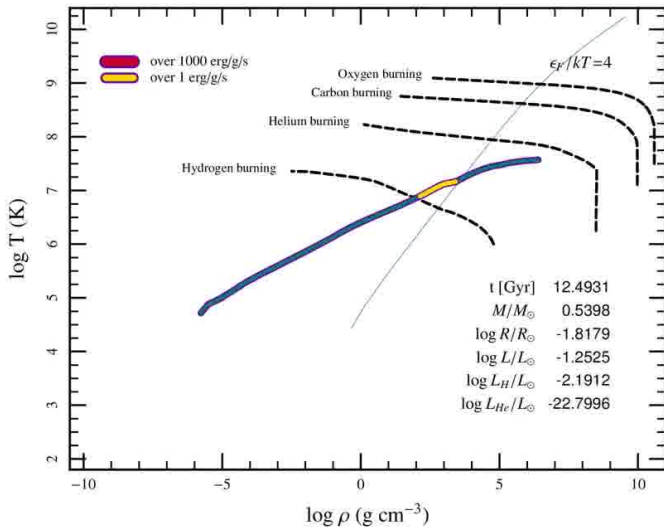
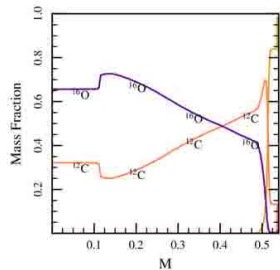
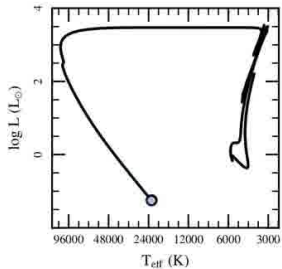
Thorsett & Chakrabarty (1999).

¹⁵e.g. a possible asteroid belt ($m < 0.05 M_\odot$) around PSR B1937+21 (Shannon et al., 2013).

The Fate of the Solar System







1. In about 5.4 Gyr from now, the Sun will evolve into a white dwarf, having a radius of $\sim 1.4 R_{\odot}$ and luminosity of $\sim 1.84 L_{\odot}$.
2. While in the main-sequence (Gough, 1981).

$$L_{\text{Sun}}(t) = \left(1 + 0.4 \left(1 - \frac{t}{t_0} \right) \right)^{-1} L_{\odot} \quad (41)$$

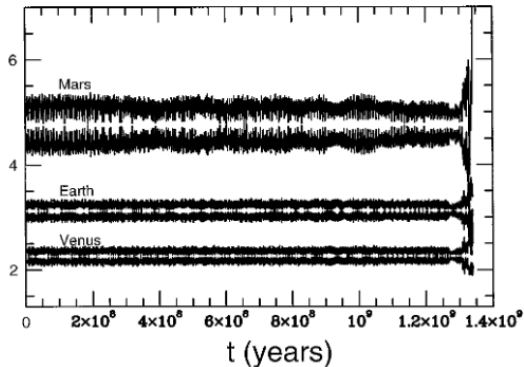
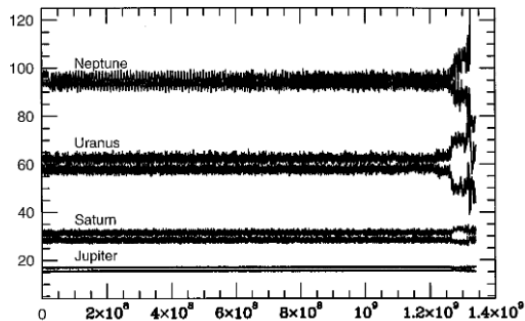
3. The Sun will reach the top of RGB with a luminosity of $2730 L_{\odot}$ and radius of $256 R_{\odot}$ ($\sim 1.19 \text{ AU}$)¹⁶

¹⁶e.g. Betelgeuse (O-type $20 M_{\odot}$ progenitor; $R = 887 \pm 203 R_{\odot}$; Dolan+2016)

3. The Sun will reach the top of RGB with a luminosity of $2730 L_{\odot}$ and radius of $256 R_{\odot}$ (~ 1.19 AU)



4. Giant planets may survive for at least 10 Gyr from the present (e.g. Duncan & Lissauer, 1998).



5. Mass loss causes the orbits of the planets to expand, while tides raised by the planets on the RGB Sun cause their orbit to decay.

Whether the Earth may survive is still debated

Schröder & Cuntz (2007) and Schröder & Smith (2007)

$$\dot{M} = 8 \times 10^{-14} M_{\odot} \text{ yr}^{-1} \frac{L(t)_{\star} R(t)_{\star}}{M(t)_{\star}} \left(\frac{T_{\text{eff}}}{4000 \text{ K}} \right)^{3.5} \left(\frac{1 + g_{\odot}}{4300 g(t)_{\star}} \right) \quad (42)$$

The Sun may lose $0.332 M_{\odot}$ when it reaches the top of the RGB $\therefore a_{\oplus} = 1.5 \text{ AU}$.

On the other hand, when it reaches the top of the RGB, the Sun will have **virtually stopped spinning**, exerting a torque on Earth with a typical value of

$$\Gamma = -3.3 \times 10^{26} \text{ kg m}^2 \text{ s}^{-2}, \quad (43)$$

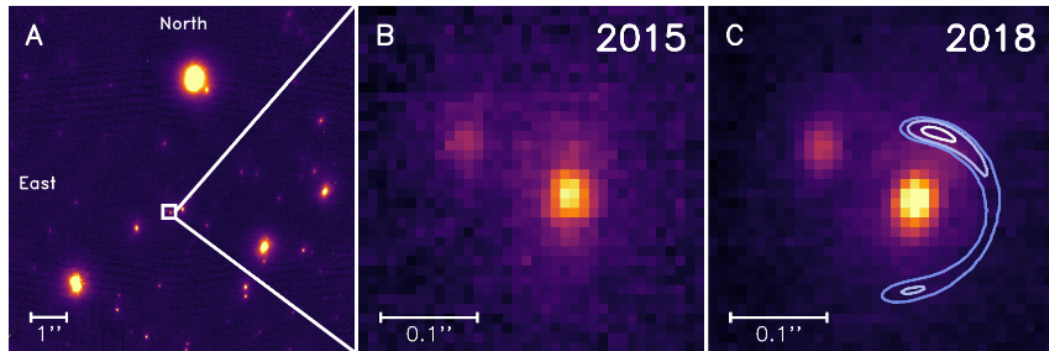
which is sufficient to dump Earth into the Sun's expanded envelope, despite the Sun's mass loss.

In general, planets beyond ~ 5 AU (around solar-type stars) may survive during the post-main-sequence evolution (Debes & Sigurdsson, 2002).

Whether or not the Earth may be engulfed in a few G-yr does not matter. Life will end long before this.

A mere 10% increase in the Solar flux will likely cause a rapid loss of Earth's oceans via photolysis of water in the stratosphere followed by the escape of the hydrogen to space (Kasting, 1998). Catastrophic ocean loss could occur in about **200 Myr**. Even if humans manage to survive this calamity, we will find it uncomfortable when the continued increase in the Sun's luminosity tips Earth's atmosphere into a runaway greenhouse state, and the former biosphere of Earth comes to resemble the surface of Venus.

MOA-2010-BLG-477Lb ($1.4 M_{\text{Jup}}$ at about 2.8 AU; Blackman et al., 2021)



Sanderson et al., (2022), *Can Gaia find planets around white dwarfs?* $\rightarrow 8 \pm 2$ **exoplanets.**

